Crystal Structure Refinement and Single Crystal ^{81}Br Zeeman NQR Study of $KHgBr_3 \cdot H_2O$

Hiromitsu Terao[1], Tsutomu Okuda[2], Sachiyo Uyama[1], Hisao Negita[2], Shi-qi Dou[3], Hartmut Fuess[3], and Alarich Weiss †

[1] Faculty of Integrated Arts and Sciences, Tokushima University, Minamijosanjima-cho, Tokushima 770, Japan

[2] Department of Chemistry, Faculty of Science, Hiroshima University, Kagamiyama, Higashihiroshima 739, Japan

[3] Fachbereich Materialwissenschaft, Technische Hochschule Darmstadt, Petersenstr. 20, D-64287 Darmstadt, Germany

Z. Naturforsch. **51 a,** 1197–1202 (1996); received June 14, 1996

Three ^{81}Br NQR resonance lines of $KHgBr_3 \cdot H_2O$ were detected between 77 K and room temperature. From the Zeeman effect measurement on a single crystal the nuclear quadrupole coupling constants (e^2qQ/h) and the asymmetry parameters (η) were obtained, which are 228.42 MHz and 0.005, 226.24 MHz and 0.005, and 108.76 MHz and 0.465 for e^2qQ/h and η at 295 K, respectively. Large deviations of the observed directions of electric field gradient tensors from the directions expected from previous X-ray results have been found. With the present X-ray redetermination, ^{81}Br NQR and structure are in good agreement. The structure and bonding in the compound are discussed.

Key words: $KHgBr_3 \cdot H_2O$, X-Ray analysis, NQR, Crystal structure, Chemical bonding.

Introduction

It is well known that mercury(II) halogenides HgX_2 (X=Cl, Br, I) interact with alkali metal halogenides and substituted ammonium halogenides etc. to form a variety of complex compounds containing anion units such as HgX_3^-, HgX_4^{2-}, and $Hg_2X_5^-$. [e. g. 1 - 4]. Widely different structure types of anions have been found, ranging from isolated anions to infinite chain polyanions. Thus, the coordination of the Hg(II) atom is also variable, though it tends to be preferably linear in chlorides and trigonal or tetrahedral in bromides and in iodides [3]. In addition, in case of lower coordination numbers such as two or three the coordination tends to be completed by additional longer contacts between the Hg(II) atoms and the ligands X. Consequently tetrahedral, trigonal bipyramidal, and octahedral environments result around the Hg(II) atoms. The variety of coordination of Hg(II) is related to the closed d-shell structure and the relatively large radius of Hg(II) [3, 4]. The nuclear quadrupole resonance (NQR) frequency is a sensitive function of the electronic state around the relevant nucleus [5]. The halogen NQR investigation of mercury(II) halide complexes may thus be helpful for understanding the coordination as well as the bonding in these crystals.

The crystal structure of $KHgBr_3 \cdot H_2O$ has already been determined by Padmanabhan and Yadava [6]. The structure belongs to orthorhombic symmetry ($Cmc2_1$, $Z = 4$) with $a = 437$, $b = 1687$, and $c = 1014$ pm. In the structure, a mercury atom is surrounded by four bromine atoms in an irregular tetrahedron. Each tetrahedron shares two corners, resulting in a zigzag chain of Br-Hg-Br-Hg atoms along the a-axis. It has seemed rather eccentric that the bridging bond Hg-Br_b is shorter than the terminal bonds Hg-Br_t as shown in the structure.

In order to elucidate the structure and bonding in this substance we have observed the ^{81}Br NQR lines and the Zeeman effect for those with a single crystal. The Zeeman effect results have exhibited large deviations in the directions of electric field gradient (EFG)

Presented at the XVIth Congress and General Assembly International Union of Crystallography, Beijing, China, August 21 - 29, 1993.

Reprint requests to Dr. Hiromitsu Terao.

0932-0784 / 96 / 1200-1197 $ 06.00 © – Verlag der Zeitschrift für Naturforschung, D-72072 Tübingen

Table 1. Experimental conditions for the crystal structure determination and crystallographic data of $KHgBr_3 \cdot H_2O$. Diffractometer: Stoe-Stadi 4; wavelength: 71.069 pm (MoK_α); Monochromator: Graphite (002); Scan $\omega/2\theta$. $M = 486.3$.

Crystal habit	Colorless, needles
Size/$(mm)^3$	$0.045 \times 0.13 \times 1.9$
Absorption coeff. (μ/m^{-1})	37000
$(\sin\theta/\lambda)_{max} \times 10^5$/pm	0.0065
Reflections measured:	1506
symmetry independent:	832
considered:	796
Number of free parameters:	37
$F(000)$	856
$R(F)$	0.087
$R_w(F)$	0.085
$R_m(F)$	0.101
Lattice constants a/pm	436.5(2)
b/pm	1689.6(5)
c/pm	1015.0(4)
$V_{Ucell} \times 10^{-6}/(pm)^3$	748.57(86)
Space group	$C_{2v}^{12} - Cmc2_1$
Formula units/Unit cell Z	4
$\rho_{calc}/mg \cdot m^{-3}$	4.41(1)
$\rho_{obs}/mg \cdot m^{-3}$	4.40(1)
Point positions	Atoms Hg, $Br^{(1)}$, $Br^{(2)}$, $Br^{(3)}$, K, O in 4a: $0, y, z$; $0, -y, z + 1/2$.

tensors from those expected in the structure of Padmanabhan and Yadava [6]. Therefore, we have done the structure redetermination by X-ray analysis.

Experimental

$KHgBr_3 \cdot H_2O$ crystals were obtained by cooling a hot aqueous solution which contains a slight excess of KBr to $HgBr_2$. The crystalline needles obtained were dried over silica gel in a desiccator. The powder X-ray pattern of the compound was coincident with that described in [7]. A large single crystal for the Zeeman-effect measurement was grown in a glass ampule by the Bridgman method. The outer diameter of the ampoule was 12 mm; one end was tapered to a capillary. The sample crystals were sealed into the ampule together with their mother liquor. In the high-temperature upper part of the Bridgman furnace whose temperature was kept at about 368 K, the content was dissolved leaving a few of small single crystals in the tip of the ampoule. After descending the ampule towards the low-temperature part of the furnace with a speed of about 4 mm a day, a single crystal, about 3 cm long, was grown. It was freed from mother liquor and dried over silica gel in a desiccator. For the single crystal X-ray diffraction experiment, small single crystals were selected.

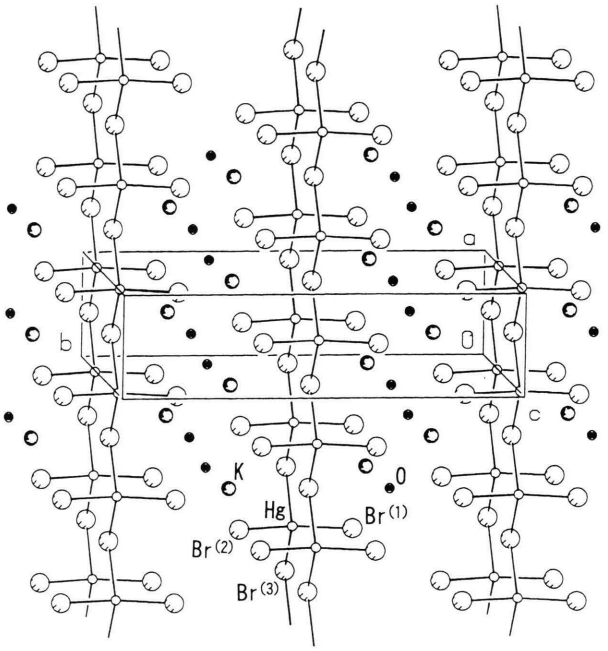

Fig. 1. The unit cell of $KHgBr_3 \cdot H_2O$. Heavily distorted $HgBr_4$ tetrahedra exist which are linked at two corners resulting in infinite chains along the a-axis.

The NQR spectra were observed by using a superregenerative detector. The sample crystals produced many piezoelectric lines, this effect became more serious with decreasing temperature. On the Zeeman-effect experiment zero-splitting cones were searched on an oscilloscope at room temperature (20 - 25°C). The magnetic fields up to 2×10^{-2} T were applied by using a goniometer described in [8].

The crystal structure was determined by single crystal methods with a 4-circle diffractometer. From the collected diffraction intensities, after appropriate corrections of absorption and Lorentz-polarization factor, the structure was determined by direct methods [9] and refined by least squares methods [10]. In Table 1 the experimental conditions for the structure determination are given.

Results

Figure 1 shows the unit cell of $KHgBr_3 \cdot H_2O$ in an overall view according to our X-ray result. Due to the heavy atoms Hg and Br we could not locate the hydrogen atoms. The crystal belongs to the orthorhombic space group $Cmc2_1$, with $Z = 4$ formula units in the

Atom	*x/a*	*y/b*	*z/c*	U_{11}	U_{22}	U_{33}	U_{23}
Hg	0.0000	–0.0032(1)	0.8607(1)	440(14)	180(10)	819(20)	53(19)
$Br^{(1)}$	0.0000	0.1405(3)	0.9188(6)	432(49)	221(26)	273(52)	–15(21)
$Br^{(2)}$	0.0000	0.1434(3)	0.4384(7)	344(41)	224(24)	296(42)	–36(20)
$Br^{(3)}$	0.0000	0.4980(3)	0.6823(6)	294(30)	216(27)	356(27)	– 1(25)
K	0.0000	0.3038(8)	0.1848(17)	247(57)	468(78)	435(62)	27(66)
O	0.0000	–0.2945(50)	0.1873(98)	478(290)			

Table 2. Positional and thermal parameters of the atoms in the unit cell of $KHgBr_3 \cdot H_2O$. Except for the O atom, the temperature factor is of the form $T = \exp(-2^2(U_{11}h^2a^{*2} + U_{22}k^2b^{*2} + U_{33}l^2c^{*2} + 2U_{12}hka^*b^* + 2U_{13}hla^*c^* + 2U_{23}klb^*c^*))$; because of the special position of all atoms in x, U_{12} and U_{13} are set zero. The isotropic temperature factor was adopted for the O atom.

Table 3. Intra- and interatomic distances and angles in the structure of $KHgBr_3 \cdot H_2O$. The distances d are given in pm and the angles in degree.

Connection	*d*/pm	Connection	Angle/°
$Hg\text{-}Br^{(1)}$	249.7(5)	$Br^{(1)}\text{-}Hg\text{-}Br^{(2)'}$	148.0(2)
$Hg\text{-}Br^{(2)}$	249.7(5)	$Br^{(1)}\text{-}Hg\text{-}Br^{(3)'}$	98.3(1)
$Hg\text{-}Br^{(3)'}$	283.6(4) (twice)	$Br^{(2)'}\text{-}Hg\text{-}Br^{(3)'}$	102.0(1)
$K\cdots Br^{(1)'}$	336.1(12) (twice)	$Br^{(3)'}\text{-}Hg\text{-}Br^{(3)'}$	100.6(1)
$K\cdots Br^{(2)''}$	343.7(12) (twice)		
$K\cdots Br^{(3)''}$	334.9(13)		
K···O'	274.2(79) (twice)		
$O\cdots Br^{(1)''}$	350.6(79) (twice)		
$O\cdots Br^{(2)'''}$	351.6(79) (twice)		
$O\cdots Br^{(3)'''}$	343.9(69)		

$Br^{(1)'}$: –1/2, 1/2 – *y*, *z* – 1/2; $Br^{(1)''}$: *x*, –*y*, *z* – 1/2; $Br^{(2)'}$: *x*, –*y*, 1/2 + *z* $Br^{(2)''}$: *x* – 1/2, 1/2 – *y*, *z* – 1/2; $Br^{(2)'''}$; *x* – 1/2, *y* – 1/2, *z*; $Br^{(3)'}$; *x* – 1/2, *y* - 1/2, *z* $Br^{(3)''}$: *x*, 1 – *y*, *z* – 1/2; $Br^{(3)'''}$; *x*, –*y*, *z* – 1/2; O': *x* – 1/2, *y* + 1/2, *z*.

Table 4. ^{81}Br NQR frequencies (ν), nuclear quadrupole coupling constants (e^2qQh^{-1}), and asymmetry parameters (η) at 295 K.

	ν/MHz[a)]	e^2qQh^{-1}/MHz	η	Assignment
ν_1	114.21(46)	228.42	0.005±0.001	Terminal $Br^{(2)}$
ν_2	113.12(40)	226.24	0.005±0.001	Terminal $Br^{(1)}$
ν_3	56.31(24)	108.76	0.465±0.001	Bridging $Br^{(3)}$

a) The values in parentheses are the peak to peak *S/N* ratios observed for the powder samples on the recorder with the Zeeman-modulation. The corresponding resonance frequencies at 77 K are 117.21(90), 116.54(81), and 59.55(27) for ν_1, ν_2, and ν_3, respectively.

unit cell. The lattice constants are a = 436.5(2) pm, b = 1689.6(5) pm, and c = 1015.0(4) pm which are almost identical to the values in [6, 7]. Some crystallographic data are included in Table 1. In Table 2 we have listed the atomic coordinates and the thermal parameters. The application of anisotropic temperature factors to the O atom resulted in very large values which are probably due to the thermal motions of water molecules in the crystal. Therefore, the temperature factor of O atom was obtained isotropically, while for all other heavy atoms anisotropic temperature factors were obtained. In the crystal structure heavily distorted $HgBr_4$ tetrahedra exist which are linked at two corners, resulting in infinite chains along

Table 5. The angles (°) between the EFG axes and the crystal axes obtained from the Zeeman experiment. 1_AZ and 1_BZ denote the z components of EFG in different direction obtained for ν_1, 2_AZ and 2_BZ denote those for ν_2, and 3X, 3Y, and 3Z denote the x, y, and z components for ν_3, respectively.

Axis	1_AZ	1_BZ	2_AZ	2_BZ	3Z	3X	3Y	*a*	*b*
1_BZ	32.47								
2_AZ	4.37	28.13							
2_BZ	27.94	4.54	23.59						
3Z	16.24	16.24	11.89	11.70					
3X	106.24	73.77	101.90	78.31	90.01				
3Y	90.16	89.75	90.11	89.90	90.01	90.00			
a	90.01	89.94	90.00	90.04	90.03	90.62	0.62		
b	16.20	16.28	11.85	11.74	0.03	90.05	89.98	90.00	
c	106.19	73.72	101.84	78.25	89.95	0.63	89.37	89.99	89.99

the *a*-axis. Table 3 contains intra- and interionic distances and angles.

Three NQR lines due to ^{81}Br have been obtained in the searched range of 40 to 200 MHz, whose frequencies exhibited a normal negative temperature dependence between 77 K and room temperature. The ^{81}Br resonance lines have been confirmed by the observation of the corresponding ^{79}Br resonance lines: their frequency ratios are consistent with the ratio of the nuclear quadrupole moments $Q(^{79}Br)/Q(^{81}Br)$ = 1.19707. The ^{81}Br resonance frequencies at 295 and 77 K are listed in Table 4. The existence of three lines is consistent with two nonequivalent terminal and one bridging Br atoms in the crystal. The zero-splitting patterns obtained from the Zeeman-effect measurement are shown in Figure 2. According to the X-ray results, all Br atoms are in special positions; the terminal $Hg\text{-}Br^{(1)}$ and $Hg\text{-}Br^{(2)}$ bonds lie in the *bc* plane, and the bridging $Hg\text{-}Br^{(3)}$ bonds lie in the *ac* plane. In accordance with this situation two kinds of zero-splitting loci were obtained for $Br^{(1)}$ and $Br^{(2)}$, and only one for $Br^{(3)}$. The asymmetry parameters obtained from the zero-splitting loci are included in Table 4. It is noted that a rather large η value is allotted for ν_3. The directions of the crystal *a*-, *b*-, and *c*-axes were easily found from the two nonequivalent directions of the z components of EFG ($q_{ZZ} \equiv q$) for the respective Br_t atoms, which are the normal, the

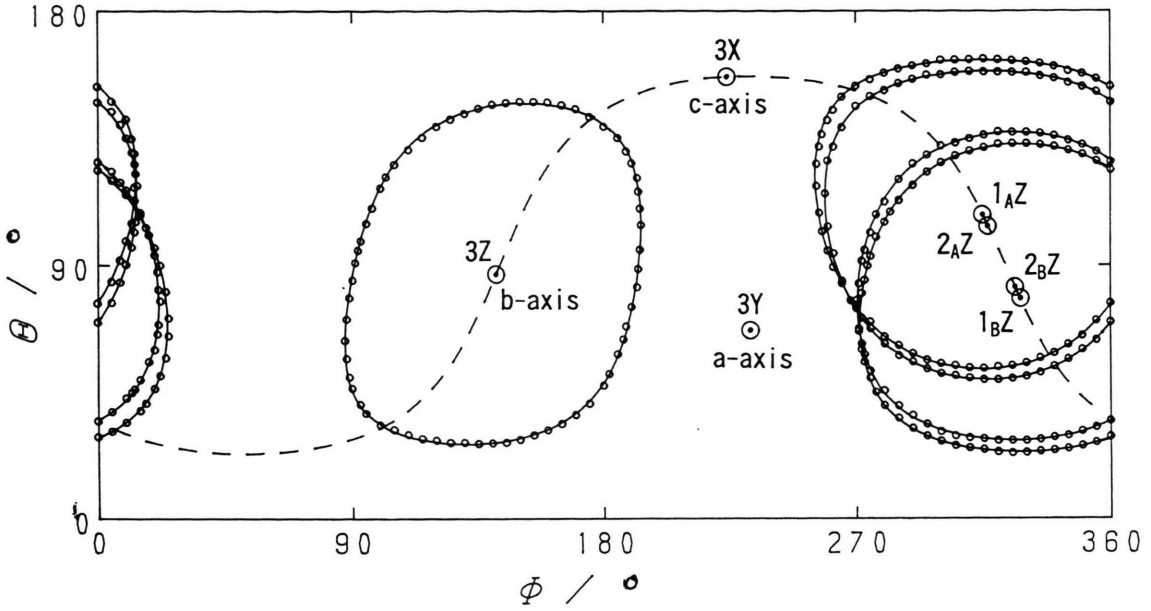

Fig. 2. The zero-splitting patterns obtained for the respective ^{81}Br NQR lines of $KHgBr_3 \cdot H_2O$. 1_AZ and 1_BZ denote the z components of EFG for ν_1, 2_AZ and 2_BZ denote those for ν_2, and 3X, 3Y, and 3Z denote the x, y, and z components for ν_3, respectively. Solid curves are the best-fitted curves for the observed points; the broken line shows the *bc* plane.

internal bisector, and the external bisector, respectively. The angles between the respective q_{ZZ} directions, which are denoted as 1_AZ, 1_BZ etc., are listed in Table 5. For the $Br^{(3)}$ atom the directions of q_{xx} and q_{yy} components of EFG, 3X and 3Y, are also included, which were obtained in high precision owing to the large distortion of its zero-splitting cones from the circular cone.

Discussion

Our X-ray results have shown the same space group and nearly the same lattice constants as found by Padmanabhan and Yadava [6]. However, the structure found differs in the atomic positions (especially of an O atom). Figure 3 shows the projection of the unit cell along [100] onto the *bc* plane. The bridging Hg-$Br^{(3)}$ bond (283.6 pm) is longer than the terminal bonds Hg-$Br^{(1)}$ (249.5 pm) and Hg-$Br^{(2)}$ (249.6 pm) differing from the former X-ray results [6]. The $HgBr_4$ tetrahedron is more severely distorted so that the terminal bond angle is 148.2° and the bridging bond angle 100.6°. These values are compared to the corresponding angles found in $CsHgBr_3$ [11], in which two different also severely distorted tetrahedra exist; terminal bond lengths are 245 - 247 pm and the bridging Hg-Br bond lengths 280 - 283 pm, and terminal bond angles are 157.3 - 159.8° and bridging bond angles 80 - 98°. Our O···Br distances 343.9 to 350.6 pm may show a possibility of hydrogen bonds, though these are fairly long compared to the corresponding distances 277 and 291 pm in [6]

The lowest-frequency ^{81}Br NQR line ν_3 is very low. It is about half of the frequencies of the other two lines (Table 4). This line exhibits a low intensity with a broad line-width. It may thus be reasonable to assign the high-frequency lines to the terminal $Br^{(1)}$ and $Br^{(2)}$ atoms and the lowest to the bridging atom $Br^{(3)}$. This assignment is also consistent with the Zeeman effect results.

It has generally been recognized that the direction of q_{ZZ} for the atom which is bonded singly to another atom in a molecule (or an ion) lies well along its bond direction [5]. The existence of the additional H-bonds, however, may turn the *z*-axes from the Hg-Br bond directions. As the intermolecular H-bonds are however thought to be fairly weak in the present crystal, deviations may remain in very small values, if any. In Table 6 the directions of q_{ZZ} for the Br_t atoms

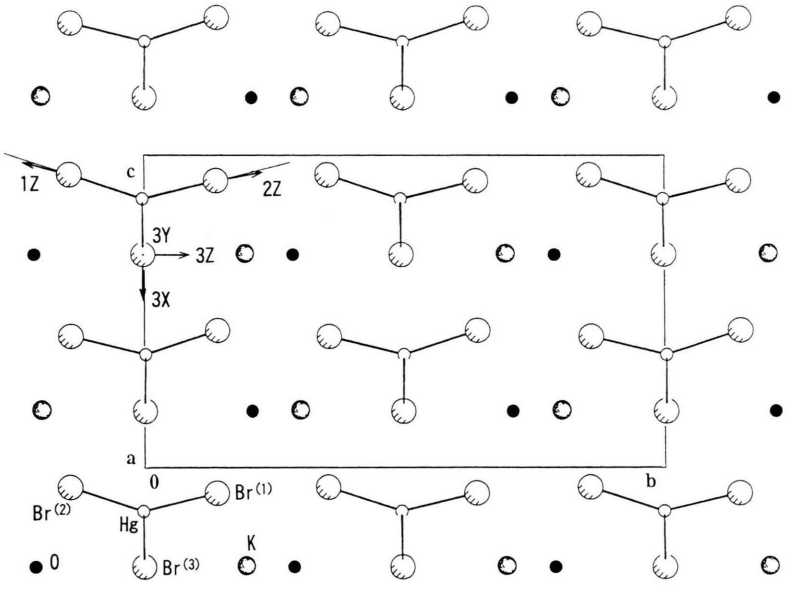

Fig. 3. The projection of the unit cell of $KHgBr_3 \cdot H_2O$ along the *a*-axis onto the *bc* plane. The EFG axes are depicted in the figure; 1Z and 2Z are tentatively assigned to $Br^{(2)}$ and $Br^{(1)}$, respectively.

Table 6. The angles (°) of the *z*-axes of EFG of terminal Br atoms with the crystallographic axes and the corresponding angles (°) of Hg-Br_t bonds from the X-ray results.

Method	Vector	*a*-axis	*b*-axis	*c*-axis
Zeeman[a]	1Z	90.00 ± 0.04	16.24 ± 0.04	73.76 ± 0.04
	2Z	90.00 ± 0.04	11.80 ± 0.06	78.23 ± 0.02
X-Ray[a]	Hg-$Br^{(1)}$	90.00	13.57	76.42
	Hg-$Br^{(2)}$	90.00	18.26	71.73
X-Ray[b]	Hg-$Br^{(1)}$	90.00	34.35	55.64
	Hg-$Br^{(2)}$	90.00	28.43	61.56

a) This work; b) [6].

Table 7. Bond Angles (°) obtained from the ^{81}Br NQR Zeeman effect and the X-ray analyses.

$Br^{(1)}$-Hg-$Br^{(2)}$	Hg-$Br^{(3)}$-Hg	Method
152.0±0.1	98.9±0.1	Zeeman[a]
148.0±0.2	100.6±0.1	X-Ray[a]
117	130	X-Ray[b]

a) This work. b) [6]; Though the respective angles 111° and 109° are listed for $Br^{(1)}$-Hg-$Br^{(2)}$ and Hg-$Br^{(3)}$-Hg in Table 4 of [6], these values are not in accordance with those calculated from the atomic coordinates. We list the latter values.

are compared with the directions of the Hg-Br_t bonds from the X-ray results. It is found that 1Z and 2Z are along the respective Hg-$Br^{(2)}$ and Hg-$Br^{(1)}$ bonds in our X-ray results within about 2°; the alternative assignment between the *z*-axes and the bond directions gives three times larger deviations of about 6°. Thus, we tentatively assign ν_1 to $Br^{(2)}$ and ν_2 to $Br^{(1)}$, respectively (Figure 3). On the other hand, these *z*-axes deviate by more than 12° from the bond directions in [6] The angles between the *z*-axes of the terminal bonds and the corresponding bond angles are listed in Table 7. Though the above coincidence between the Zeeman and our X-ray results is fairly good, the difference of 4° for the terminal bond angles seems a little larger compared to the deviations observed usually in molecular crystals [5]. Presumably this deviation may be attributed to some ionic origin and/or the hydrogen bonds in the $KHgBr_3 \cdot H_2O$ crystal.

On the other hand, the q_{XX}, q_{YY}, and q_{ZZ} axes for the $Br^{(3)}$ atom coincident well with the *c*, *a*, and *b* axes, respectively (Table 5): the *x*-axis is the bisector of the bridging angle Hg-$Br^{(3)}$-Hg lying in the *ac* plane, *y* is perpendicular to *x* in this plane, and *z* is perpendicular to the bridging bonds (Figure 3). Taking s and p orbitals into account for the bonding scheme of the bridging $Br^{(3)}$ atom, the η value is expressed as a function of the bridging angle θ [12]. The *z* and y axes alternate at the critical value of θ [13]: For $90° < \theta < 109.5°$ the *z* axis is expected to be perpendicular to the plane on which the bridging bonds (and the *y* axis) lie, and for $\theta > 109.5°$ the *z*-axis and *y*-axis alternate. The value $\theta = 130°$ in [6] predicts that the *y*-axis is perpendicular to the bridging bond Hg-$Br^{(3)}$-Hg. However, according to the Zeeman observation the perpendicular one is the *z*-axis, indicating $90° < \theta < 109.5°$. In this range of θ, the relation $\eta = -3 \cos \theta$ holds [13]. Using the observed value $\eta = 0.465$, we

obtain $\theta = 98.9°$, which agrees well with the present X-ray results (Table 7).

We may now estimate the bond orbital populations N_t and N_b for the respective terminal and bridging Br atoms according to the Townes-Dailey theory [5]. The s-hybridization is ignored for the single-bonded terminal Br atom; no correction for the distortion of the valence p orbitals by the effective nuclear charge is considered. Then, for the terminal Br_t atom

$$-(e^2qQ/h)/(e^2q_{at}Q/h) = (2 - N_t), \quad (1)$$

where the atomic quadrupole coupling constant, $e^2q_{at}Q/h$, is –643.03 MHz for ^{81}Br. On the other hand for the Br_b atom

$$-(e^2qQ/h)/(e^2q_{at}Q/h) = (1 - N_b/2)(1 + \cot^2(\theta/2)) \quad (2)$$

and

$$\eta = -3\cos\theta. \quad (3)$$

Using the e^2qQ/h and the η values in Table 4, we obtain $N_t = 1.65$ and $N_b = 1.81$, where the average value was used in the calculation for the Br_t atom. The large ionicity of the bridging bond compared to the terminal bonds coincides with the large distortion of the $HgBr_4$ tetrahedron; the anion unit may be in an intermediate situation between two extremes $(HgBr_3)^-$ and $HgBr_2 \cdot (Br)^-$.

Support by the Deutsche Forschungsgemeinschaft and the Fonds der Chemischen Industrie is gratefully acknowledged.

[1] A. F. Wells, Structural Inorganic Chemistry, 5th Ed, Clarendon Press, Oxford 1986, Chapt. 26.

[2] K.Brodersen and H. Hummel, Comprehensive Coordination Chemistry, Ed by G. Wilkinson, R. D. Gillard, and J. A. McClevertz, Pergamon Press, Oxford 1987, Vol. 5, Chapt. 2.

[3] D. Grdenic, Quart. Rev. Chem. Soc. London. **19**, 303 (1965).

[4] A. Ben Salah, J. W. Bats, H. Fuess, and A. Daoud, Inorganic Chimica Acta **63**, 169 (1982).

[5] e. g. Yu. A. Buslaev, E. A. Kravchenko, and L. Kolditz, Coordination Chem. Rev. **82**, 7 (1987); E. A. C. Lucken, Nuclear Quadrupole Coupling Constants, Academic Press, London and New York 1969.

[6] V. M. Padmanabhan and V. S. Yadava, Acta Crystallogr., Sec. B **25**, 647 (1969).

[7] R. M. Herak, L. M. Manojlovic, and S. S. Malcis, Bull. Inst. Nucl. Sci, 'Boris Kidrich7 (Belgrade) **14**, 294 (1963).

[8] H. Terao, M. Fukura, T. Okuda, and H. Negita, Bull. Chem. Soc. Japan., **56**, 1728 (1983).

[9] G. Sheldrick, SHELX86. Program for crystal structure solution, University of Gottingen, Germany 1986.

[10] G. Sheldrick, SHELX76. Program for crystal structure determination, University of Cambridge, England 1976.

[11] P. M. Fedorov and V. I. Pakhomov, Koord. Khim. **7**, 284 (1981).

[12] P. A. Casabella, P. J. Bray, and R. G. Barnes, J. Chem. Phys. **30**, 1393 (1959).

[13] C. H. Townes and A. L. Schawlow, Microwave Spectroscopy, McGraw-Hill, New York 1955.